Trends in Chemistry

CellPress REVIEWS

Review

Next-Generation Cathode Materials for Non-aqueous Potassium-Ion Batteries

Haegyeom Kim,[1,4] Huiwen Ji,[2,3,4] Jingyang Wang,[2] and Gerbrand Ceder[1,2,*]

Potassium-ion batteries have recently attracted considerable attention as cost-effective alternatives to lithium-ion batteries for large-scale energy storage. However, a major obstacle to the practical application of this emerging technology is the lack of suitable cathode materials that are capable of delivering high gravimetric/volumetric energy, stable cycle life, and high rate capability. In this review article, we review the recent progress in cathodes development for potassium-ion batteries. These materials are categorized into four types: layered oxides, Prussian blue analogs, poly-anion, and organic compounds. Based on our critical review of the reported literature, we identify poly-anion compounds as a class of promising candidates among all types and provide suggestions for future optimization.

Potassium-Ion Batteries as Next-Generation Energy Storage Systems

Despite being the dominant energy storage solution for portable electronics, lithium-ion batteries (LIBs) face challenges in terms of cost for large-scale applications, including electric vehicles and stationary storage [1]. Currently, the cost of the active cathode and anode materials in LIBs can reach nearly 40% of the total cell cost [2]. In addition, the costs are subject to resource constraints resulting from the reliance on lithium and cobalt sources for the cathode materials [1]. Compared with Li, other alkali metals such as Na and K have the advantage of being significantly less expensive (Figure 1A) [3], and their storage can often be achieved with cathode materials that do not contain resource-constrained metals [4–11].

Both Na-ion batteries (NIBs) [12–15] and K-ion batteries (KIBs) [16–19] have been actively investigated as alternative energy storage systems. In particular, KIBs are more attractive because (i) graphite can be used as the anode for KIBs (unlike for NIBs) [20]; (ii) KIB cathodes rely on almost completely different chemistries than Li-cathodes, which can lead to less expensive Co-free batteries, often based on transition-metal (TM) elements such as Fe, Mn, and V (Figure 1B); (iii) KIBs can potentially have higher voltages because the standard redox potential of K^+/K (–2.93 V versus the standard hydrogen electrode [SHE]) is comparable to that of Li^+/Li (–3.04 V versus SHE) and lower than that of Na^+/Na (–2.71 V versus SHE); in fact, the redox potential of K^+/K can be even lower than that of Li^+/Li [20]; (iv) the K^+ mobility in electrolytes is higher than that of Li^+ or Na^+ [21]; and (v) finally, less expensive Al current collectors can be used for KIBs.

However, a major challenge for the practical realization of KIBs is the identification of a suitable cathode that reversibly intercalates K^+ ions with high capacity, suitable voltage, fast kinetics, and reliable cycle life. Because the ionic radius of K^+ is significantly larger than that of Li^+, K^+ ions often stabilize different structure types than do Li^+ ions. Consequently, the corresponding cathode materials and their working voltages are expected to be different from those for LIBs. The various material types that have been developed and evaluated as cathodes for non-aqueous KIBs since 2004 (Figure 1C) fall mainly into four categories: layered oxides, Prussian blue analogs (PBAs), poly-anion oxides, and organic compounds. Their capacity and voltage

Highlights

The supply of lithium and cobalt for Li-ion battery manufacturing falls short of meeting the demand for large-scale applications, and K-ion batteries are an attractive alternative energy storage technology.

The past 5 years have witnessed an exponential increase in research on non-aqueous K-ion cathode materials. These can be categorized into four types: layered oxides, Prussian blue analogs, poly-anion, and organic compounds; however, a suitable candidate that is capable of delivering high specific energy, stable cycle life, and high rate capability is yet to be found.

Prussian blue analogs are good K-cathode candidates in terms of gravimetric energy density and have suitable voltages because of the strong interaction between K^+ ions and the metal–organic framework, which stabilizes the discharge products, but very inconsistent results are obtained across the literature due to the difficulty in controlling defects and water.

K-polyanion materials are good cathodes because of their high voltage, but not many candidates have been identified so far and thus more research for K-polyanions is required.

[1]Materials Sciences Division, Lawrence Berkeley National Laboratory, Berkeley, CA 94720, USA
[2]Department of Materials Science and Engineering, University of California, Berkeley, CA 94720, USA
[3]Energy Storage and Distributed Resources Division, Lawrence Berkeley National Laboratory, Berkeley, CA 94720, USA
[4]These authors contributed equally to this work

*Correspondence: gceder@berkeley.edu (G. Ceder).

Published by Elsevier Inc.

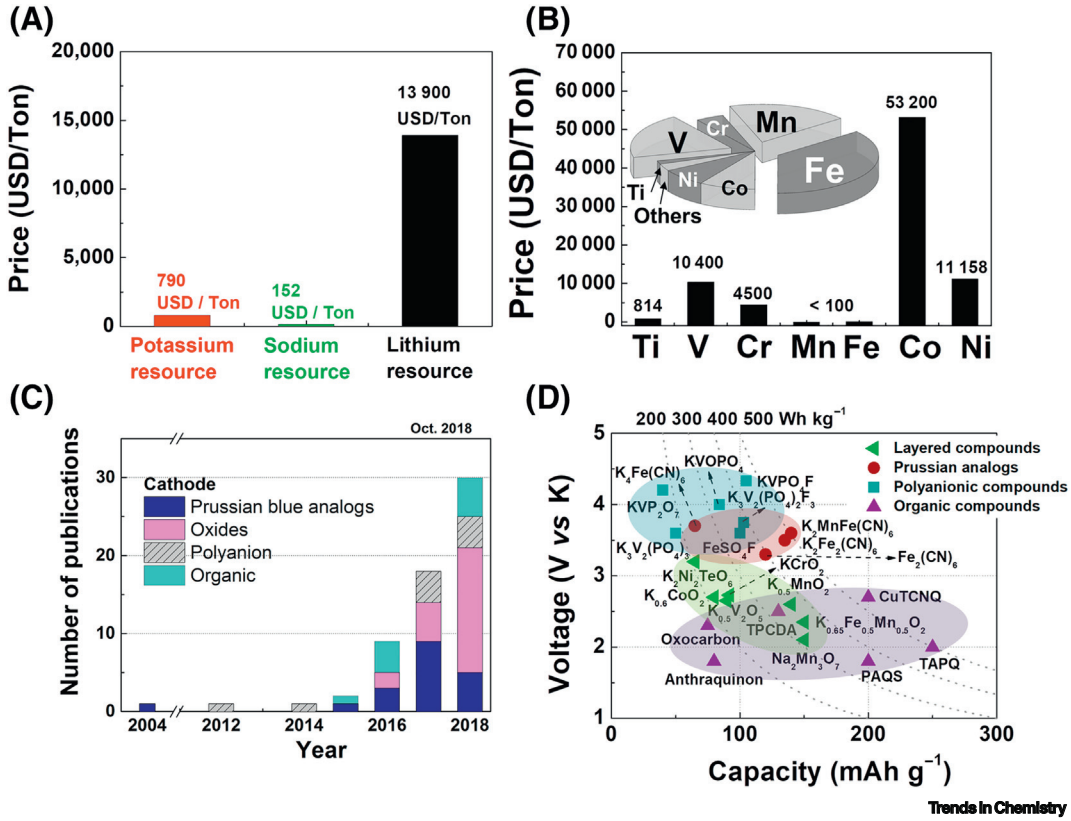

Figure 1. Price of Elements Used in Alkali-Ion Cathode Materials, Number of Publications, and Average Voltage versus Capacity Diagram of Various Types of Cathode Materials for Non-aqueous KIBs. (A) Price (USD, US dollars) of potassium, sodium, and lithium resources. US Geological Survey (USGS) Minerals Information: Commodity Statistics and Information (accessed October 2018). (B) Price (USD) of transition metal resources (Ti, V, Cr, Mn, Fe, Co, and Ni) and the relative occurrence of each transition metal in published K-ion cathodes (inset). USGS Minerals Information: Commodity Statistics and Information (accessed October 2018). (C) Number of publications per year on various cathode types (Google Scholar, accessed October 2018). (D) Capacity–voltage plots of K cathode compounds.

range are plotted in Figure 1D. Noticeably, the dominant cathode materials for LIBs are no longer the superior choice for KIBs. Instead, PBAs, which are poor-performing Li-ion cathodes, emerge as one of the major candidate material groups for KIBs when prioritized in terms of specific energy.

In this review article, we review recent progress in the development of cathode materials for non-aqueous KIBs, with the aim of stimulating further research in this rapidly growing field. We first discuss the advantages and disadvantages of each of the four cathode material types and provide perspectives and strategies for their future optimization.

Layered Oxide Compounds

Layered oxide compounds have been widely used as cathodes for LIBs and NIBs because of their high energy density achieved in these technologies. The layered oxides can be conveniently classified using an alpha-numeric expression developed by Delmas and colleagues [22]: with a letter describing the alkali site coordination (e.g., octahedral [O] or prismatic [P]) and a number referring to the oxygen stacking sequence. In a layered oxide crystal structure, the TM and alkali ions segregate into alternating slabs, forming a 2D open framework for the fast migration of alkali ions, including the large K^+ ions, making them likely candidates for K storage compounds.

$K_{0.3}MnO_2$ was the first layered compound demonstrated as a suitable cathode for K storage [23]. It adopts a distorted P2-type structure with orthorhombic symmetry (space group: *Cmcm*). When cycled between 1.5 and 4.0 V, the material delivers a reversible capacity of ~125 mAh g^{-1}. Since then, many more layered K-cathodes have emerged. For example, Kim and colleagues developed a P3-type $K_{0.5}MnO_2$ cathode that showed a reversible capacity of ~110 mAh g^{-1} between 1.5 and 3.9 V [5]. Significant capacity increase to ~140 mA h g^{-1} was observed when cycled to a higher upper cutoff voltage of 4.2 V, yet accompanied by fast capacity decay. The K_xCoO_2 reported by Kim and colleagues [24] and Hironaka and colleagues [25] shows two structure types (i.e., P2 and P3) depending on the starting alkali content (x = ~0.4 and ~0.6, respectively). The P2-type K_xCoO_2 shows a stair-like charge/discharge profile, indicating the occurrence of multiple phase transitions upon K de/intercalation (Figure 2A), as confirmed by *in situ* X-ray diffraction (XRD) characterization. Hironaka and colleagues demonstrated that the voltage curves of K_xCoO_2 are not significantly affected by the oxygen stacking sequence (P2 versus P3) of the as-synthesized pristine material [25]. Instead, both groups argue that the voltage profiles are dominated by K^+/vacancy ordering. Recently, a P2-type $K_2Ni_2TeO_6$ cathode was reported by Masese and colleagues [26]. This material has a high average discharge voltage of ~3.3 V but

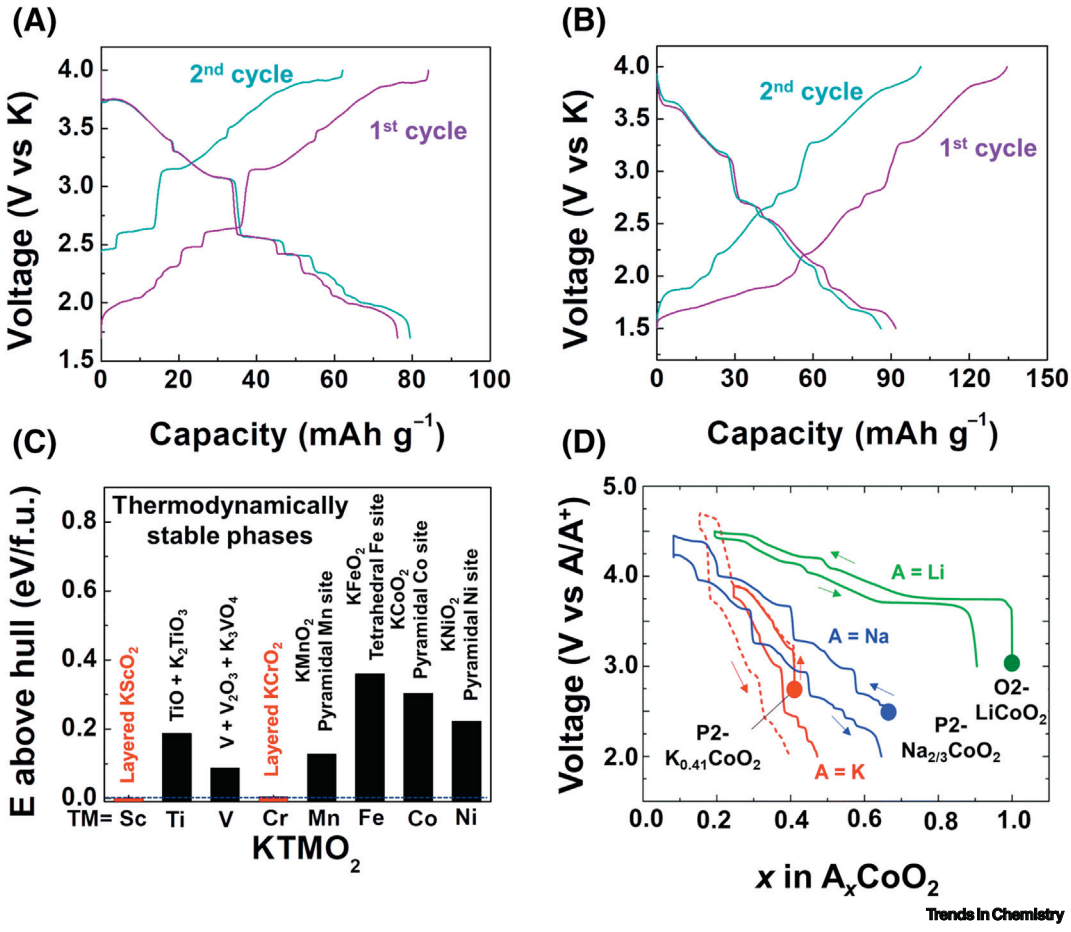

Figure 2. Charge–Discharge Profiles and Computed Stability of Typical Layered Oxide Compounds. (A) Charge–discharge profiles of P2-$K_{0.6}CoO_2$. Reproduced, with permission, from [24]. (B) Charge–discharge profiles of O3-$KCrO_2$. Reproduced, with permission, from [27]. (C) Computed stability of layered KMO_2 compounds. Energy above the hull for various O3-layered compounds with KMO_2 stoichiometry. The height of the bar is the driving force for conversion to the more stable phases listed. Reproduced, with permission, from [27]. (D) Comparison of charge–discharge profiles for $K_{0.41}CoO_2$, $Na_{0.67}CoO_2$, and $LiCoO_2$. Reproduced, with permission, from [25].

a low reversible capacity of ~65 mAh g^{-1}. The authors attributed the high working voltage to the electro-negative TeO_6^{6-} moieties. The effect of mixed TMs on cathode performance has also been investigated. These mixed-TM oxides (i.e., $K_xFe_{0.5}Mn_{0.5}O_2$) [4] deliver higher specific capacity than single-TM oxides (e.g., K_xMnO_2 and K_xCoO_2). Nevertheless, no significant improvement in the energy density was observed because of the decrease in the operating voltage.

One of the major issues with layered oxides is that almost all of them are K deficient, limiting the amount of K that they can bring into a K cell. In this context, the stoichiometric O3-type $KCrO_2$ developed by Kim and colleagues is remarkable as it is the only layered oxide material that can be synthesized without K deficiency [27]. A stoichiometric O3-type $KCrO_2$ shows a reversible capacity of ~93 mAh g^{-1} with an average voltage of ~2.73 V (Figure 2B) [27]. The unique stability of $KCrO_2$ in the layered structure (Figure 2C) was explained using *ab initio* calculations. By evaluating the thermodynamic stability of various stoichiometric KMO_2 compounds (Figure 2C), Kim and colleagues [27] found that the strong unscreened K^+–K^+ interactions destabilize the layered structure for most stoichiometric KMO_2 compounds and instead favor other 3D structures. However, the strong octahedral site preference of Cr^{3+} can overcome the penalty of the K^+–K^+ interactions, thereby uniquely stabilizing $KCrO_2$ in the layered structure.

Another major drawback of layered K-compounds is their much steeper voltage curves with many more voltage steps compared to those of corresponding Li and Na systems (Figure 2D) [25]. For example, although O2-$LiCoO_2$ exhibits a flat voltage profile [25,28], a steeper voltage profile with multiple steps is observed for P2-$Na_{2/3}CoO_2$. These slope features become even more apparent in P2-$K_{0.41}CoO_2$. P2-Na_xCoO_2 exhibits eight voltage steps between $Na_{0.1}CoO_2$ and $Na_{0.65}CoO_2$ that, on average, equals one voltage step for every 0.069 Na^+ ion intercalated, whereas P2-K_xCoO_2 has seven voltage steps between $K_{0.2}CoO_2$ and $K_{0.5}CoO_2$, equaling one voltage step for every 0.043 K^+ ion intercalated. The underlying mechanism is that as the alkali ions become larger, the increasing inter-slab distance prevents the oxygen anions from effectively screening the alkali–alkali repulsion, leading to a stronger interaction between them. Such strong and long-ranged repulsive interactions cause a remarkable number of phase transitions between various ordered K^+-vacancy configurations, as well as large voltage slope. The relation between voltage slope and interaction can be seen by taking the derivative of $V(x) = -\mu_K(x) \approx \frac{\delta E}{\delta x}$, where x represents the amount of K [29]. In a mean field or regular solution approach, $\Delta E_{mix} = \omega x(1 - x)$ and hence $\frac{\delta V(x)}{\delta x} \approx -2\omega$, where ω is proportional to the effective K^+–K^+ interaction [30]. Even in systems where the intercalating ions are not randomly distributed, the overall slope remains proportional to the interaction. The large voltage slope limits the usable capacity within a given voltage window.

In addition, the upper cutoff voltage allowed for most K-layered oxides is limited due to the structural instability and the concomitant capacity loss at deep charge [5,23–25,27]. For example, when depotassiating K_xMnO_2 and K_yCrO_2 to $x < 0.2$ and $y < 0.4$, respectively, the crystallinity of electrodes is significantly reduced [5,27] as confirmed by *ex situ* XRD. The origin of this irreversible structural change at low K contents is currently unclear and should be further investigated to enable the use of a wider K de/intercalation range.

Prussian Blue Analogs

PBAs have received considerable attention as K-cathode materials because of their long cycle life, inexpensive TM components, and potentially scalable synthesis. Their 3D open frameworks (Figure 3A) host reversible redox reactions by allowing the insertion/extraction of alkali ions. The composition of a PBA can be expressed as $K_xM_A[M_B(CN)_6]_{1-\delta}{\cdot}nH_2O$, where M_A and M_B denote the N-coordinated and C-coordinated TM ions, respectively, and δ and n denote the contents of

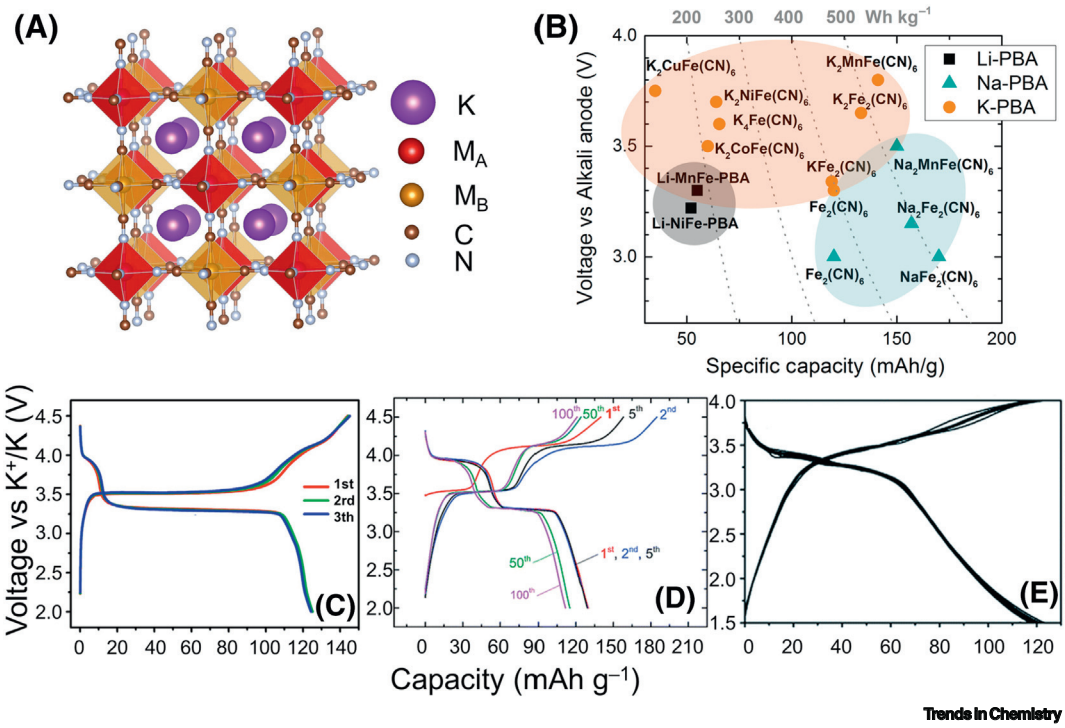

Figure 3. Crystal Structure, Average Voltage versus Gravimetric Capacity, and Voltage Profiles of Prussian Blue Analogs (PBAs). (A) Crystal structure of PBAs. (B) Voltage–capacity relation of Li-, Na-, and K-PBA cathode materials [8–10,33–39]. Voltage profiles of (C) $K_{0.61}Fe[Fe(CN)_6]_{0.91}{\cdot}0.32H_2O$. Reproduced, with permission, from [44]. (D) $K_{1.64}Fe[Fe(CN)_6]_{0.89}{\cdot}0.15H_2O$. Reproduced, with permission, from [34]. (E) A K-deficient $FeFe(CN)_6$ phase. Reproduced, with permission, from [10].

$[M_B(CN)_6]$ vacancies and residual water, respectively. Initially, PBAs were used as both anode and cathode in aqueous electrolytes [31]; however, the limited variation of redox potential that can be realized in PBAs leads to a limited battery voltage. In 2004, Eftekhari first demonstrated the use of electrochemically deposited $KFe[Fe(CN)_6]$ as a K-cathode in a nonaqueous electrolyte, achieving a high voltage of ~3.7 V (versus K^+/K) and a reasonable capacity of ~0.9 K^+/formula unit (f.u.) [32].

The specific capacity of K-PBAs is slightly lower than that of Na-PBAs because of the heavier K^+ ions; nevertheless, their higher voltages result in competitive specific energies (Figure 3B) [8–10, 33–39]. There are two known factors that contribute to the voltage difference: (i) the lower anode potential for K^+/K than for Na^+/Na; and (ii) according to density functional theory [40], the interaction between alkali ions and the metal–organic framework strengthens with alkali size, thereby stabilizing the discharged products and resulting in an increasing intercalation potential from Li^+ to Na^+ to K^+. The voltages of Li-PBAs are comparable to those of Na-PBAs, most likely because of the cancellation of these two effects. The increased voltage with increasing ionic radius of intercalating species may also explain why $Co^{2+/3+}$ is redox active for Na-PBAs but has a redox potential above the upper stability window of non-aqueous electrolytes for K-PBAs [33]. Thus, the only K-PBAs capable of delivering a capacity larger than 1 K^+/f.u. at reasonably high voltage are either Fe based or Mn based [11,34].

The electrochemical performance of PBAs is highly sensitive to lattice defects. A PBA can theoretically insert/extract 2 K^+/f.u., corresponding to a theoretical capacity of ~156 mAh g^{-1}. However, the $[Fe(CN)_6]$ vacancies and residual water negatively affect the electrochemical performance. The former reduces the available electron reservoir, and the latter leads to side reactions and low coulombic efficiency. For example, $K_{0.220}Fe[Fe(CN)_6]_{0.805}{\cdot}4.01H_2O$, which has a

high vacancy and water content as a result of its rapid precipitation synthesis, delivers a capacity of ~0.84 K^+/f.u. with low initial coulombic efficiency of 44% [41]. Slow crystallite nucleation and post-synthesis drying seem critical for better performance [42]. A similar study comparing the effect of crystallinity on performance in Na-PBAs concluded that defects lead to slow kinetics and poor cycle life [43].

Such sensitivity to defects leads to significant inconsistencies across the literature. A wide spectrum of synthesis methods and conditions have been reported, yielding varied electrochemical results even for the same PBA system. Chong and colleagues reported moderate rate performance for nanosized $KFe[Fe(CN)_6]_{0.82}{\cdot}2.87H_2O$ prepared using hydrothermal synthesis [9]. In contrast, Shadike and colleagues reported superior rate capability for a K-deficient phase $FeFe(CN)_6$ (the actual composition was not reported) synthesized using a simple precipitation method [10]. This high rate capability was tentatively attributed to the minimal structural deformation during cycling. The voltage profiles also vary. $K_{0.61}Fe[Fe(CN)_6]_{0.91}{\cdot}0.32H_2O$ reported by Zhu and colleagues has a significantly longer discharge plateau at 3.28 V than at 3.95 V (Figure 3C) [44]; in contrast, $K_{1.64}Fe[Fe(CN)_6]_{0.89}{\cdot}0.15H_2O$ reported by Bie and colleagues shows two equally long discharge plateaus at 3.8 and 3.15 V (Figure 3D) [34]; and the K-deficient $FeFe(CN)_6$ phase reported by Shadike and colleagues has two almost overlapping plateaus at 3.3 and 3.2 V (Figure 3E) [10]. No real satisfactory explanations for these variations have been provided so far.

Such confusion is in fact not uncommon in the field of metal–organic frameworks, where routine measurements such as powder XRD provide limited structural information to explain the observed variation in properties [45]. In-depth characterization of the nature of the defects using theory and experiments and their correlation with electrochemical performance is urgently needed. This understanding needs to be paired with study of how synthetic conditions influence composition and defects to increase reproducibility and future optimization/commercialization of this class of materials.

Polyanionic Compounds

Polyanionic compounds have also been investigated as high-voltage cathodes for KIBs. Recham and colleagues demonstrated reversible K de/intercalation in polyanion compounds [46]. They first extracted ~0.9 K^+/f.u. from a $KFeSO_4F$ electrode by using Li/$KFeSO_4F$ cells. The depotassiated material was subsequently evaluated in K/$FeSO_4F$ cells and ~0.8 K^+/f.u. could be reintercalated at an average voltage of ~3.6 V. Later, an extensive screening of known K-containing compounds in the K-M-O and K-M-P-O space was conducted by Park and colleagues based on several criteria, including [47] the material contains oxidizable TM species (e.g., Ti, V, Cr, Mn, Fe, Co, Ni, and Mo) in octahedral sites; the material has 1D K^+ transport channels with large void space (>1.8 Å); and the theoretical capacity is larger than 80 mAh g^{-1}. The screening identified 10 candidates, including KMP_2O_7 (M = Ti, V, Cr, Fe, Mo), $KM(PO_3)_3$ (M = Ni, Co), $K_2(VO_3)(P_2O_7)_2$, $K_2MnP_2O_7$, and $KMnVO_4$. Among them, only KMP_2O_7 (M = Ti, V, and Mo) shows reversible capacity during galvanostatic cycling: $KTiP_2O_7$ and $KMoP_2O_7$ have limited capacities (~20 mAh g^{-1}) and low average voltages (<3.0 V) even at 50°C, whereas KVP_2O_7 exhibits reasonable electrochemical performance, delivering ~55 mAh g^{-1} at ~4.2 V (Figure 4A) [47]. The structural evolution of KVP_2O_7 during cycling detected using *in situ* and *ex situ* XRD suggested a reversible two-phase reaction between the monoclinic KVP_2O_7 and the triclinic $K_{0.4}VP_2O_7$. Recently, two new high-voltage cathodes, $KVPO_4F$ and $KVOPO_4$, were investigated by Chihara and colleagues [48], which achieved capacities of ~92 and 84 mAh g^{-1} with average voltages of ~4.13 and ~4.0 V, respectively. The average voltage and capacity of $KVPO_4F$ were further improved by Kim and colleagues to ~4.33 V and ~105 mAh g^{-1}, respectively, through the synthesis of a highly stoichiometric compound (Figure 4B) [49]. Their structure analysis using XRD, X-ray absorption spectroscopy, and

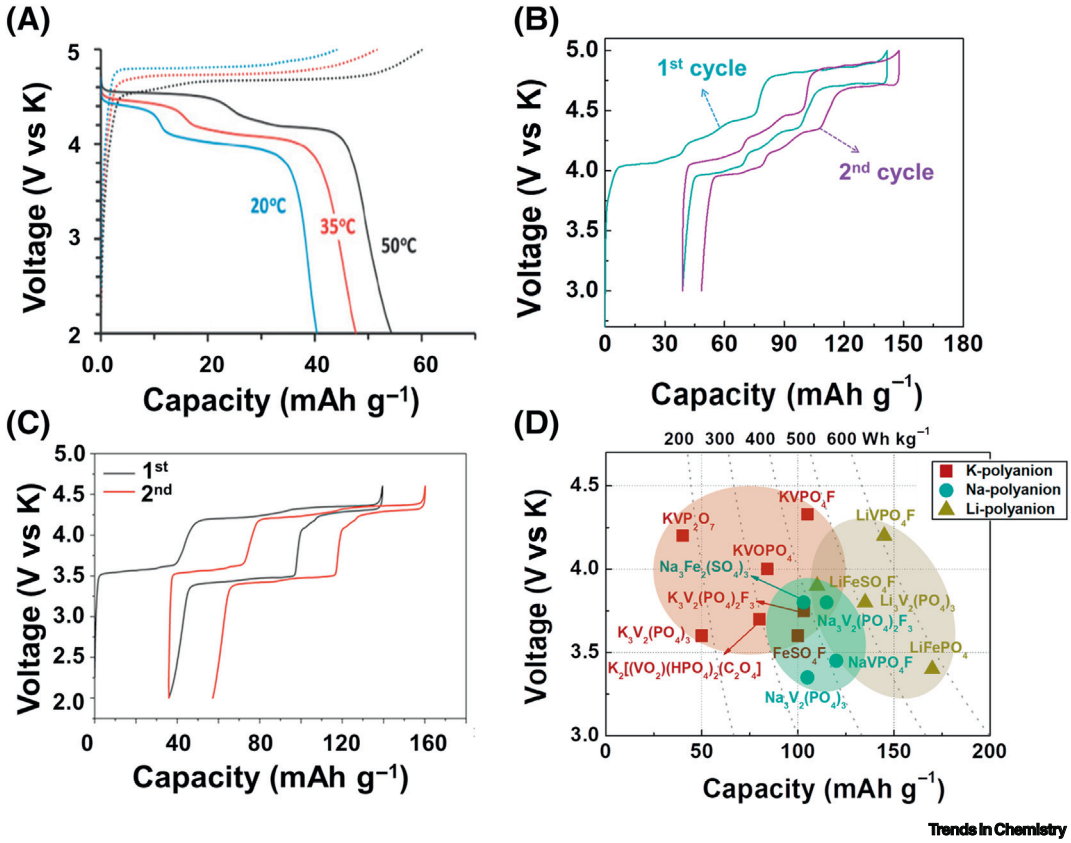

Figure 4. Charge–Discharge Profiles and Capacity-Voltage Plot of K Polyanionic Compounds. (A) KVP_2O_7, reproduced, with permission, from [47]. (B) $KVPO_4F$, reproduced, with permission, from [49]. (C) $K_3V_2(PO_4)_2F_3$, reproduced, with permission, from [50]. (D) Voltage–capacity plots of Li-, Na-, and K-polyanion cathode materials [46–60].

nuclear magnetic resonance spectroscopy showed that oxygen substitution on F sites in $KVPO_4F$ induces anion disordering, thus reducing the working voltage and specific capacity. Their findings suggest that the material prepared by Chihara and colleagues [48] was likely an oxygen-substituted $KVPO_{4+x}F_{1-x}$ compound, thereby explaining the origin of its lower voltage and capacity than a stoichiometric $KVPO_4F$. Kim and colleagues thus proposed that the synthesis of stoichiometric $KVPO_4F$ is crucial to achieving high voltage and capacity.

Metastable K-containing polyanionic compounds have also been obtained and evaluated. A $K_3V_2(PO_4)_2F_3$ cathode was prepared via electrochemical Na^+/K^+ exchange from a NASICON-type $Na_3V_2(PO_4)_2F_3$ by Lin and colleagues [50]. *In situ* XRD and *ex situ* energy-dispersive X-ray spectroscopy analysis revealed the complete replacement of Na^+ ions with K^+ ions after five cycles. The *in situ*–formed $K_3V_2(PO_4)_2F_3$ cathode provides a reversible capacity of ~103 mAh g^{-1}, corresponding to ~1.8 K^+/f.u., with an average voltage of ~3.75 V (Figure 4C). The performance is similar to that of $Na_3V_2(PO_4)_2F_3$, which de/intercalates 2 Na^+/f.u. at an average voltage of 3.8 V [51]. An attempt to directly synthesize $K_3V_2(PO_4)_2F_3$ by using a conventional solid-state method was not successful [50].

In general, most polyanionic compounds provide higher voltages (>3.5 V versus K/K^+) than Na-analogs and are even comparable to some Li-analogs [46–60], with some materials cycling at over 4.0 V versus K/K^+ (i.e., KVP_2O_7, $KVPO_4F$, and $KVOPO_4$) as shown in Figure 4D [47–49].

The high voltage of polyanionic compounds can be attributed to three factors: (i) the inductive effect of the electro-negative polyanion moieties; (ii) a 3D K arrangement with larger K^+–K^+ distances compared to that in layered oxides, which reduces the effective K^+–K^+ interaction; and (iii) a 3D framework in which the volume change associated with K-insertion is spread out between all three dimensions, unlike in layered materials where it is largely accommodated by slab-space expansion, which compromises the screening of K^+–K^+ interaction. It is worth noting that the third factor may not be present when the polyanion compound has a layered structure that can easily relax perpendicular to the layer. However, the specific capacity of many K-polyanionic compounds is still far below Li- and Na-counterparts. We propose that new polyanionic K-cathodes that enable double redox reactions (e.g., $Mn^{2+/4+}$, $V^{3+/5+}$, and $Ni^{2+/4+}$) should be developed to increase the theoretical electron reservoir.

Organic Compounds

Organic compounds are considered attractive candidates for KIBs by some because of their low cost and flexible structures. The argument made is that weak intermolecular interaction more easily accommodates deformations upon inserting large K^+ ions. 3,4,9,10-Perylene-tetracarboxylic acid-dianhydride (PTCDA) was first demonstrated by Chen and colleagues as a cathode material and exhibits a capacity of 131 mAh g^{-1} in the voltage range of 1.5–3.5 V, corresponding to the insertion of 2 K^+/f.u. [61]. Xing and colleagues evaluated the structural evolution of PTCDA by using *ex situ* XRD [62] and showed that the material undergoes a high degree of amorphization upon potassiation with its crystallinity only partially restored when re-charged. We suspect that this loss of long-range order is responsible for the poor cycling stability, although it is not exactly clear why amorphization would reduce capacity. In addition, *ex situ* infrared spectra reveals electron injection into C=O bonds and the formation of potassium enolate groups during the potassiation process. However, the authors suggested that the redox process is better described by a molecular orbital or doping analogy because of the delocalized nature of the injected electrons. Jian and colleagues studied poly(anthraquinonyl sulfide) as another cathode material for KIBs [63]. This compound shows a high reversible capacity of 200 mAh g^{-1} and good cycling performance with 75% of the initial capacity retained after 50 cycles at a rate of C/10. A series of oxocarbon salts with the formula $K_2(CO)_n$ (n = 4, 5, 6) were investigated by Zhao and colleagues as KIB cathodes [64]. These materials deliver a capacity of 212 mAh g^{-1} at 0.2C and 164 mAh g^{-1} at 10C, and the two-electron reaction mechanism of the carbonyl group was confirmed by *in situ* Raman measurements. Very recently, copper-tetracyanoquinodimethane (CuTCNQ) was proposed as a cathode material for KIBs with a discharge capacity of 244 mAh g^{-1} at an average discharge potential of 2.7 V, using both redox-active $Cu^{+/2+}$ and $TCNQ^{2-/0}$ [65]. However, it should be noted that, in this work, the $TCNQ^{2-/0}$ redox process is accompanied by anion insertion from electrolytes, rendering the material unsuitable for realizing practical rocking-chair-type KIBs because the anions in the electrolytes are cycled during battery operation. In summary, the rich and versatile chemistry of organic compounds can potentially offer a cost-efficient solution for KIBs; however, several issues must be properly addressed: the low volumetric energy density and low operating voltage of most organic systems will have to be compensated by other benefits achieved when using organic cathodes. Dissolution of organic species from the cathode in conventional organic electrolytes result in poor capacity retention. In addition, organic cathodes themselves usually do not contain K^+ ions; therefore, the need for a pre-potassiation process or the use of a K metal anode are additional drawbacks for their practical application.

Concluding Remarks and Future Perspectives

In Figure 5, the gravimetric energy is plotted versus the volumetric energy of various K-cathode compounds, including layered compounds, Prussian blue analogs, polyanionic compounds,

Outstanding Questions

Is there another structure type beyond the existing four (i.e., layered oxides, Prussian blue analogs, poly-anion, and organic compounds) that can achieve higher energy density for reversible insertion/extraction of K ions?

What is the origin of capacity fading for layered K-ion cathodes at high voltages and can it be mitigated?

Are there other layered oxides that can be synthesized without K deficiency, besides $KCrO_2$?

What is the precise role of water in Prussian blue cathodes during cycling and can the water content be reproducibly controlled?

Can the compositional and structural space of polyanionic cathode materials be further expanded? By far, the small handful of polyanionic cathode materials share very similar crystal structures and have limited compositional flexibility. The majorities of K-containing polyanionic compounds have the transition metal species taking a redox-inactive tetrahedral coordination and are therefore unsuitable to be used as cathode materials.

Organic cathode materials that contain the mobile alkali ion before cycling have been realized for Li-ion batteries, but not for K-ion batteries. Can such pre-potassiated organic compounds be synthesized to enable the use of graphite anode for practical application?

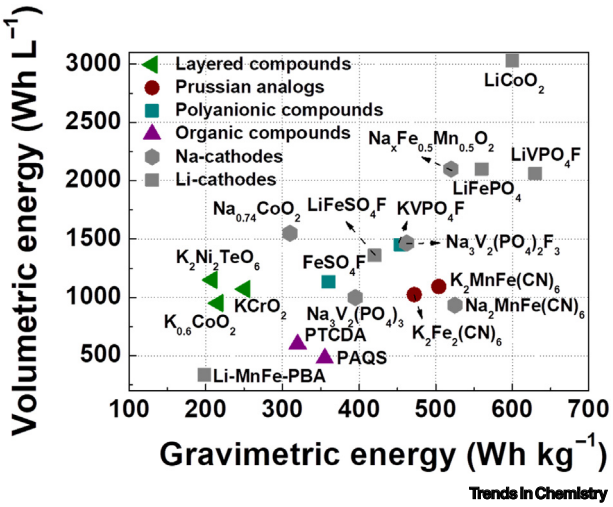

Figure 5. Gravimetric versus Volumetric Energy Density of K-Cathode Compounds. (See [11,24,26,27,35,39,46,49,57,60,61,63,66–71].)

and organic compounds with comparison to Li- and Na-cathode materials [11,24,26,27,35,39,46,49,57,60,61,63,66–71]. A few K-cathode materials (e.g., $KVPO_4F$) [49] exhibit comparable gravimetric and volumetric energies to Na-cathode materials. However, most of the K-cathodes still have lower energy content, especially volumetrically, than Li- or Na-cathode materials.

The large ionic radius of K^+ leads to very different structural requirements for cathode materials than for Li^+. Layered oxide compounds, which have a 2D arrangement of K^+ ions, poorly screen the strong K^+–K^+ interactions, resulting in a significantly more sloped voltage profile and lower specific energy (<300 Wh kg^{-1}) than Li- or Na-based layered oxides. In contrast, PBAs and polyanionic compounds have 3D K^+ arrangements, which can effectively reduce K^+–K^+ interactions. Therefore, PBAs and polyanionic compounds have flatter voltage profiles and higher average working voltage and thus deliver higher gravimetric energy. For example, $KVPO_4F$ provides ~450 Wh kg^{-1} and $K_2MnFe(CN)_6$ delivers ~510 Wh kg^{-1} [11,49]. These examples indicate that PBAs and polyanionic compounds are promising material classes in which to find better cathodes with high specific energy. Likewise, any search for new materials should focus on 3D structures. Some important challenges are listed in the Outstanding Questions.

Future endeavors in optimizing PBA and polyanionic structures should focus on addressing their specific limitations. Despite the high gravimetric energy (>450 Wh kg^{-1}) of PBAs, they exhibit low volumetric energy density (<1200 Wh L^{-1}). Some investigation in the role of the interstitial water molecules in PBAs is needed as its content is difficult to precisely control, and it remains unclear how the interstitial water molecules in PBAs lead to deterioration of their capacity with cycling. We expect that polyanionic compounds are better options for KIB cathodes. They have higher volumetric energy density and less complex structures and fewer defects (i.e., interstitial water and TM vacancy in the structure) than PBAs. Although several K-polyanionic compounds with high working voltage (>3.5 V) have been developed, their energy density is not yet sufficient to compete with most Li and Na cathodes. To increase the energy density of KIBs, K polyanionic cathodes that can enable double redox reactions (i.e., $Mn^{2+/4+}$, $V^{3+/5+}$, and $Ni^{2+/4+}$) should be developed to increase the achievable specific capacity. Given that polyanionic compounds are generally high in voltage, strategies to optimize the working potential in order to fully use double

redox in a practical voltage window are needed, for example, tuning the inductive effect by tailoring the polyanionic groups, or tailoring the site energy of K^+.

Acknowledgments

This work was supported by the Battery Innovative Contest program of LG Chem, Ltd. under contract 20181787. H.K.'s contribution was also supported by the Basic Science Research Program through the National Research Foundation of Korea funded by the Ministry of Education (2017R1A6A3A03001850). H.J.'s contribution was supported by the Assistant Secretary of Energy Efficiency and Renewable Energy, Vehicle Technologies Office of the U.S. Department of Energy under Contract No. DE-AC02-05CH11231.

References

1. Olivetti, E.A. *et al.* (2017) Lithium-ion battery supply chain considerations: analysis of potential bottlenecks in critical metals. *Joule* 1, 229–243
2. Chung, D. *et al.* (2015) *Automotive Lithium-Ion Battery Supply Chain and U.S. Competitiveness Considerations,* Clean Energy Manufacturing Analysis Center
3. USGS Minerals Information: Commodity Statistics and Information (2018) *US Geological Survery*, National Minerals Information Center
4. Wang, X. *et al.* (2017) Earth abundant Fe/Mn-based layered oxide interconnected nanowires for advanced K-ion full batteries. *Nano Lett.* 17, 544–550
5. Kim, H. *et al.* (2017) Investigation of potassium storage in layered P3-type $K_{0.5}MnO_2$ cathode. *Adv. Mater.* 29, 1702480
6. Deng, T. *et al.* (2018) Layered P2-type $K_{0.65}Fe_{0.5}Mn_{0.5}O_2$ microspheres as superior cathode for high-energy potassium-ion batteries. *Adv. Funct. Mater.* 28, 1800219
7. Zhao, S. *et al.* (2019) Construction of hierarchical $K_{1.39}Mn_3O_6$ spheres via AlF_3 coating for high-performance potassium-ion batteries. *Adv. Energy Mater.* 9, 1803757
8. Pei, Y. *et al.* (2018) Low-cost $K_4Fe(CN)_6$ as a high-voltage cathode for potassium-ion batteries. *ChemSusChem* 11, 1285–1289
9. Chong, S. *et al.* (2017) Potassium ferrous ferricyanide nanoparticles as a high capacity and ultralong life cathode material for nonaqueous potassium-ion batteries. *J. Mater. Chem. A* 5, 22465–22471
10. Shadike, Z. *et al.* (2017) Long life and high-rate Berlin green $FeFe(CN)_6$ cathode material for a non-aqueous potassium-ion battery. *J. Mater. Chem. A* 5, 6393–6398
11. Xue, L. *et al.* (2017) Low-cost high-energy potassium cathode. *J. Am. Chem. Soc.* 139, 2164–2167
12. Kim, H. *et al.* (2016) Recent progress in electrode materials for sodium-ion batteries. *Adv. Energy Mater.* 6, 1600943
13. Kim, S.-W. *et al.* (2012) Electrode materials for rechargeable sodium-ion batteries: potential alternatives to current lithium-ion batteries. *Adv. Energy Mater.* 2, 710–721
14. Chevrier, V.L. and Ceder, G. (2011) Challenges for Na-ion negative electrodes. *J. Electrochem. Soc.* 158, A1011–A1014
15. Palomares, V. *et al.* (2012) Na-ion batteries, recent advances and present challenges to become low cost energy storage systems. *Energy Environ. Sci.* 5, 5884–5901
16. Kim, H. *et al.* (2018) Recent progress and perspective in electrode materials for K-ion batteries. *Adv. Energy Mater.* 8, 1702384
17. Wu, X. *et al.* (2017) Emerging non-aqueous potassium-ion batteries: challenges and opportunities. *Chem. Mater.* 29, 5031–5042
18. Pramudita, J.C. *et al.* (2017) An initial review of the status of electrode materials for potassium-ion batteries. *Adv. Energy Mater.* 7, 1602911
19. Eftekhari, A. *et al.* (2017) Potassium secondary batteries. *ACS Appl. Mater. Interfaces* 9, 4404–4419
20. Komaba, S. *et al.* (2015) Potassium intercalation into graphite to realize high-voltage/high-power potassium-ion batteries and potassium-ion capacitors. *Electrochem. Commun.* 60, 172–175
21. Okoshi, M. *et al.* (2017) Theoretical analysis of interactions between potassium ions and organic electrolyte solvents: a comparison with lithium, sodium, and magnesium ions. *J. Electrochem. Soc.* 164, A54–A60
22. Delmas, C. *et al.* (1980) Structural classification and properties of the layered oxides. *Physica B+C* 99, 81–85
23. Vaalma, C. *et al.* (2016) Non-aqueous K-ion battery based on layered $K_{0.3}MnO_2$ and hard carbon/carbon black. *J. Electrochem. Soc.* 163, A1295–A1299
24. Kim, H. *et al.* (2017) K-ion batteries based on a P2-type $K_{0.6}CoO_2$ cathode. *Adv. Energy Mater.* 7, 1700098
25. Hironaka, Y. *et al.* (2017) P2- and P3-K_xCoO_2 as an electrochemical potassium intercalation host. *Chem. Commun.* 53, 3693–3696
26. Masese, T. *et al.* (2018) Rechargeable potassium-ion batteries with honeycomb-layered tellurates as high voltage cathodes and fast potassium-ion conductors. *Nat. Commun.* 9, 3823
27. Kim, H. *et al.* (2018) Stoichiometric layered potassium transition metal oxide for rechargeable potassium batteries. *Chem. Mater.* 30, 6532–6539
28. Yabuuchi, N. *et al.* (2013) A comparative study of $LiCoO_2$ polymorphs: structural and electrochemical characterization of O2-, O3-, and O4-type phases. *Inorg. Chem.* 52, 9131–9142
29. Aydinol, M.K. and Ceder, G. (1997) First-principles prediction of insertion potentials in Li-Mn oxides for secondary Li batteries. *J. Electrochem. Soc.* 144, 3832–3835
30. Bevan Ott, J. and Boerio-Goates, J. (2000) Preface to the two-volume series: chemical thermodynamics: principles and applications and chemical thermodynamics: advanced applications. In *Chemical Thermodynamics: Principles and Applications* (Ott, J.B. and Boerio-Goates, J., eds), pp. xv–xix, Academic Press
31. Jayalakshmi, M. and Scholz, F. (2000) Charge–discharge characteristics of a solid-state Prussian blue secondary cell. *J. Power Sources* 87, 212–217
32. Eftekhari, A. (2004) Potassium secondary cell based on Prussian blue cathode. *J. Power Sources* 126, 221–228
33. Wu, X. *et al.* (2017) Prussian white analogues as promising cathode for non-aqueous potassium-ion batteries. *Electrochem. Commun.* 77, 54–57
34. Bie, X. *et al.* (2017) A novel K-ion battery: hexacyanoferrate(ii)/graphite cell. *J. Mater. Chem. A* 5, 4325–4330
35. Song, J. *et al.* (2015) Removal of interstitial H_2O in hexacyanometallates for a superior cathode of a sodium-ion battery. *J. Am. Chem. Soc.* 137, 2658–2664
36. Wang, B. *et al.* (2018) Prussian blue analogs for rechargeable batteries. *iScience* 3, 110–133
37. Wang, L. *et al.* (2015) Rhombohedral prussian white as cathode for rechargeable sodium-ion batteries. *J. Am. Chem. Soc.* 137, 2548–2554
38. Mizuno, Y. *et al.* (2012) Precise electrochemical control of ferromagnetism in a cyanide-bridged bimetallic coordination polymer. *Inorg. Chem.* 51, 10311–10316
39. Okubo, M. *et al.* (2010) Switching redox-active sites by valence tautomerism in Prussian blue analogues $A_xMn_y[Fe(CN)_6]\cdot nH_2O$ (A: K, Rb): robust frameworks for reversible Li storage. *J. Phys. Chem. Lett.* 1, 2063–2071
40. Ling, C. *et al.* (2013) First-principles study of alkali and alkaline earth ion intercalation in iron hexacyanoferrate: the important role of ionic radius. *J. Phys. Chem. C* 117, 21158–21165
41. Zhang, C. *et al.* (2017) Potassium Prussian blue nanoparticles: a low-cost cathode material for potassium-ion batteries. *Adv. Funct. Mater.* 27, 1604307
42. He, G. and Nazar, L.F. (2017) Crystallite size control of Prussian white analogues for nonaqueous potassium-ion batteries. *ACS Energy Lett.* 2, 1122–1127

43. You, Y. *et al.* (2014) High-quality Prussian blue crystals as superior cathode materials for room-temperature sodium-ion batteries. *Energy Environ. Sci.* 7, 1643–1647
44. Zhu, Y.-H. *et al.* (2018) High-energy-density flexible potassium-ion battery based on patterned electrodes. *Joule* 2, 736–746
45. Hafizovic, J. *et al.* (2007) The Inconsistency in adsorption properties and powder XRD data of MOF-5 is rationalized by framework interpenetration and the presence of organic and inorganic species in the nanocavities. *J. Am. Chem. Soc.* 129, 3612–3620
46. Recham, N. *et al.* (2012) Preparation and characterization of a stable $FeSO_4F$-based framework for alkali ion insertion electrodes. *Chem. Mater.* 24, 4363–4370
47. Park, W.B. *et al.* (2018) KVP_2O_7 as a robust high-energy cathode for potassium-ion batteries: pinpointed by a full screening of the inorganic registry under specific search conditions. *Adv. Energy Mater.* 8, 1703099
48. Chihara, K. *et al.* (2017) $KVPO_4F$ and $KVOPO_4$ toward 4 volt-class potassium-ion batteries. *Chem. Commun.* 53, 5208–5211
49. Kim, H. *et al.* (2018) A new strategy for high-voltage cathodes for K-ion batteries: stoichiometric KVPO4F. *Adv. Energy Mater.* 8, 1801591
50. Lin, X. *et al.* (2019) $K_3V_2(PO_4)_2F_3$ as a robust cathode for potassium-ion batteries. *Energy Storage Mater.* 16, 97–101
51. Zhu, C. *et al.* (2017) A high power–high energy $Na_3V_2(PO_4)_2F_3$ sodium cathode: investigation of transport parameters, rational design and realization. *Chem. Mater.* 29, 5207–5215
52. Liao, J. *et al.* (2019) A vanadium-based metal–organic phosphate framework material $K_2[(VO)_2(HPO_4)_2(C_2O_4)]$ as a cathode for potassium-ion batteries. *Chem. Commun.* 55, 659–662
53. Han, J. *et al.* (2017) Investigation of $K_3V_2(PO_4)_3$/C nanocomposites as high-potential cathode materials for potassium-ion batteries. *Chem. Commun.* 53, 1805–1808
54. Jian, Z. *et al.* (2013) Superior electrochemical performance and storage mechanism of $Na_3V_2(PO_4)_3$ cathode for room-temperature sodium-ion batteries. *Adv. Energy Mater.* 3, 156–160
55. Jin, T. *et al.* (2017) Electrospun $NaVPO_4F$/C nanofibers as self-standing cathode material for ultralong cycle life Na-ion batteries. *Adv. Energy Mater.* 7, 1700087
56. Barpanda, P. *et al.* (2014) A 3.8-V earth-abundant sodium battery electrode. *Nat. Commun.* 5, 4358
57. Kang, B. and Ceder, G. (2009) Battery materials for ultrafast charging and discharging. *Nature* 458, 190
58. Zheng, J.-C. *et al.* (2012) Novel synthesis of $LiVPO_4F$ cathode material by chemical lithiation and postannealing. *J. Power Sources* 202, 380–383
59. Huang, H. *et al.* (2002) Nanostructured composites: a high capacity, fast rate $Li_3V_2(PO_4)_3$/carbon cathode for rechargeable lithium batteries. *Adv. Mater.* 14, 1525–1528
60. Ati, M. *et al.* (2011) Synthesis and electrochemical properties of pure $LiFeSO_4F$ in the triplite structure. *Electrochem. Commun.* 13, 1280–1283
61. Chen, Y. *et al.* (2015) Organic electrode for non-aqueous potassium-ion batteries. *Nano Energy* 18, 205–211
62. Xing, Z. *et al.* (2016) A perylene anhydride crystal as a reversible electrode for K-ion batteries. *Energy Storage Mater.* 2, 63–68
63. Jian, Z. *et al.* (2016) Poly(anthraquinonyl sulfide) cathode for potassium-ion batteries. *Electrochem. Commun.* 71, 5–8
64. Zhao, Q. *et al.* (2016) Oxocarbon salts for fast rechargeable batteries. *Angew. Chem. Int. Ed.* 55, 12528–12532
65. Ma, J. *et al.* (2018) Endowing CuTCNQ with a new role: a high-capacity cathode for K-ion batteries. *Chem. Commun.* 54, 5578–5581
66. Berthelot, R. *et al.* (2010) Electrochemical investigation of the P_2–Na_xCoO_2 phase diagram. *Nat. Mater.* 10, 74
67. Yabuuchi, N. *et al.* (2012) P2-type $Na_x[Fe_{1/2}Mn_{1/2}]O_2$ made from earth-abundant elements for rechargeable Na batteries. *Nat. Mater.* 11, 512
68. Jian, Z. *et al.* (2012) Carbon coated $Na_3V_2(PO_4)_3$ as novel electrode material for sodium ion batteries. *Electrochem. Commun.* 14, 86–89
69. Barker, J. *et al.* (2005) Structural and electrochemical properties of lithium vanadium fluorophosphate, $LiVPO_4F$. *J. Power Sources* 146, 516–520
70. Bianchini, M. *et al.* (2015) Comprehensive investigation of the $Na_3V_2(PO_4)_2F_3$–$NaV_2(PO_4)_2F_3$ system by operando high resolution synchrotron x-ray diffraction. *Chem. Mater.* 27, 3009–3020
71. Ohzuku, T. and Ueda, A. (1994) Solid-state redox reactions of $LiCoO_2$ ($R\bar{3}m$) for 4 volt secondary lithium cells. *J. Electrochem. Soc.* 141, 2972–2977